Snow Penetration Depth Inversion in Tibetan Plateau Based on Coherence Scattering Model with X-band Data

Lihong Deng[1], Xing Peng [1], Qinghua Xie [1], Yushan Zhou[2], Lijun Shen [1]

[1] The School of Geography and Information Engineering, China University of Geosciences (Wuhan), Wuhan 430074, China
[2] School of Geosciences and Info-Physics, Central South University, Changsha 410083, China

Keywords: InSAR, Coherence scattering model, Snow depth, Tibetan plateau, TSX/TDX.

Abstract

The snow penetration depth is a necessary input parameter to accurately evaluate the thickness and vertical structure of snow layer, which is conducive to understanding the freeze-thaw process of ice and snow and predicting the change of ice and snow mass balance. Interferometric Synthetic Aperture Radar (InSAR) exhibits great potential in estimating snow penetration depth due to the emission of microwave band and the ability of operating under all-day and all-weather conditions. In previous studies, the penetration depth of snow was obtained based on InSAR coherence, but the external factors such as temperature, humidity, topography, dielectric constant and so on also affect the penetration dept. In order to extract the penetration depth in detail, this paper this paper adopts a uniform volume model as the basis, introduces two parameters describing the physical properties of snow: the volume ambiguity height and the volumetric decorrelation. Then, the magnitude of volumetric decorrelation is used to establish the internal relationship between the magnitude and the volume ambiguity height to estimate the snow penetration depth. In order to verify the effectiveness and feasibility of this method, a TSX/TDX InSAR pair covering southeast Tibetan Plateau in 2012 is applied to estimate the snow penetration depth. And results indicate that X-band penetration depths range mainly between-2.753 meters and -4.589 meters with an average value of -3.671 meters m and standard deviation of 0.918 meters in snowy regions on the plateau.

1. Introduction

Snow is an important component of the cryosphere, with significant impacts on hydrology, climate, ecology, and human activities and livelihoods(Eppler and Rabus 2022; Patil et al. 2020). The active remote sensing technique has a good application in obtaining the internal vertical structure of snow within extensive snow-covered areas, due to its advantages of penetrating ability to ground objects and large-scale observation(Mahmoodzada et al. 2020). The penetration depth of microwaves in snow serves as a parameter for evaluating the vertical structure within the snowpack, thereby assisting in the quantitative estimation of snow accumulation. This information plays a crucial role in monitoring snowmelt runoff, water resource management, and other related applications(Benedikter et al. 2022; Li et al. 2021).

Interferometric Synthetic Aperture Radar (InSAR), as one of the main methods of active remote sensing to acquire ground information, can obtain millimeter-level information only by interferometric processing of two SAR images, holding significant potential for acquiring snow penetration depth(Zhang et al. 2023; Zhao et al. 2024). Over the past few decades, numerous researchers have extensively investigated the application of InSAR for estimating snow penetration depth. Some studies proposed a method to extract the penetration depth from the volumetric decorrelation to obtain the penetration depth, and successfully calculated the penetration depth in the Antarctic region's X-band to be approximately -4.3 to -5.8 meters(Rott et al. 2021). Other studies calculated the penetration depth of P-band in the areas surrounding Mt. St. Helens and Mt. Rainier snow based on InSAR coherence, and the result is -9.2m(Xu et al. 2023). Therefore, the method based on coherence for acquiring penetration depth is feasible. It is well known that the longer the radar wavelength, the better the penetration capability, but external factors such as temperature, humidity, terrain, dielectric constant, etc. can also have an impact on the penetration depth results.(Rizzoli et al. 2017b; Zhou et al. 2022) Therefore, relying solely on coherence for obtaining penetration depth is insufficient for precise depth calculation. Given this, this paper constructs a coherence scattering model that considers external factors such as snow properties to refine the extraction of penetration depth.

When the microwave penetration into the interior of the scatterer will produce refraction and scattering, the penetration depth value is included in this part of the scattering and refraction, as shown in Figure.1. To describe this process, the paper introduces two parameters: the volume ambiguity heigh and the volumetric decorrelation. The volume ambiguous height within the scatterer serves as a conversion factor between coherence and penetration depth, incorporating the dielectric properties of snow. And the volumetric decorrelation due to internal scattering within the scatterer, capturing the vertical structural information of the scatterer. Ultimately based on the above two parameters containing the physical properties of the snowpack, this paper uses the UV model to describe the vertical structure of snow, constructs the volumetric decoherence expression of snow, and then obtains the unique corresponding relationship between coherent magnitude and coherent phase. Finally calculates the depth of snow penetration by combining the magnitude and volume ambiguity height. This process is the construction of a coherence scattering model. This article presents the first application of the method in the snowy region regions of the Tibetan Plateau. A pair of TSX/TDX InSAR data over the southeastern Tibetan Plateau in 2012 was collected to estimate the penetration depth of snow. Analyzed were the correlations between external variables like climate, topography, and dielectric constants, and parameters in interferometric measurements, aiming to comprehend the influences on

penetration depth.

The structure of the following sections is as follows: Section 2 presents the study area and experimental data, providing a detailed overview of the principles of the coherence scattering model. Section 3 showcases and analyzes the experimental results. Finally, in Section 4, summarizes the content of this paper.

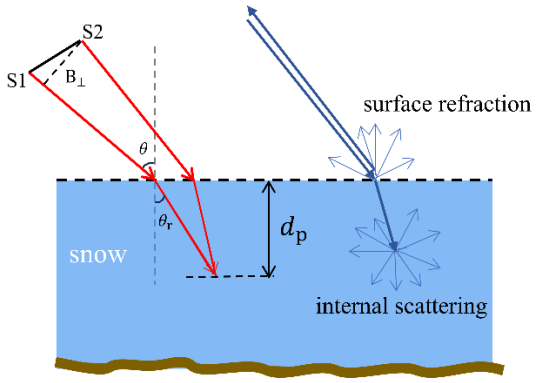

Figure 1. Schematic of microwave penetration through snow

2. Materials and Methods

2.1 Study Area

The Tibetan Plateau is the largest plateau in the world with extensive glaciers and one of the primary regions in China with significant snow accumulation. The Zuhuixue Glacier and the surrounding glacier complex in the southeastern part of the Tibetan Plateau (94°28′-94°53′N, 31°38′-31°56′E) were selected for this study, as illustrated in Figure 2.

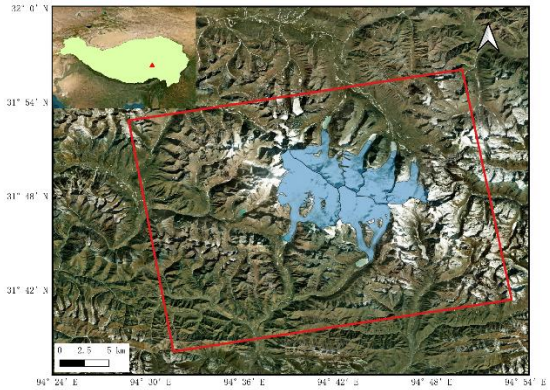

Figure 2. Geographic location of the TerraSAR-X image (indicated by the red box), with the study area (blue area).

According to The Second Glacier Inventory Dataset of China (CGI-2)(Guo et al. 2015), the total area of this glacier complex is about 670km^2, with the highest elevation at about 6200 meters and the lowest elevation at about 4190 meters. The average annual temperature in the area is below 0°C, indicating a cold climate, the snow glaciers do not melt all year round, and the number of days of annual snow cover can be more than 200 days. Due to low winter precipitation and temperatures, there is minimal melting, making it favorable for snow monitoring in this region. In order to exclude external influences and analyze the internal characteristics of snow more comprehensively, this paper will focus on glacier clusters composed of glaciers with an area larger than 90km^2 (such as Zuhuixue Glacier, etc.), the blue-covered area in Figure 2.

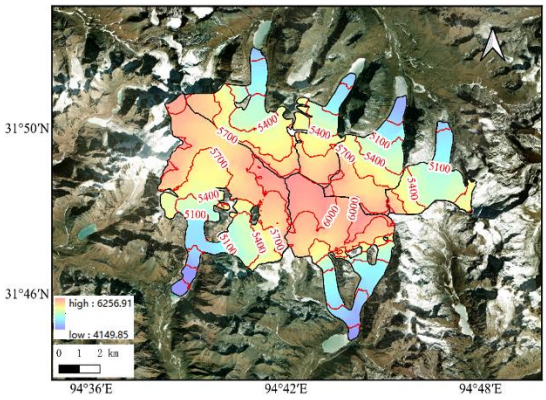

Figure 3. DEM and contours of the study area.

2.2 Datasets

The TerraSAR-X and TanDEM-X dual-satellite formation X-band single-polarization (HH) SAR data on November 14, 2012 were selected for this study. The azimuth resolution is 1.98 meters, the range resolution is 1.36 meters, the incidence angle is 34.80°, and the vertical baseline is 119.21 meters. The experiment utilized GAMMA for operations such as image registration, interferometry, terrain phase removal, and coherence extraction.

2.3 The Coherence Scattering Model

The penetration depth is defined as the one-way distance when the microwave penetrates the scatterer losing power attenuation of 1/e, which can be expressed as formula (1).

$$d_p = \frac{\cos\theta_v}{2\sigma} \quad (1)$$

Where d_p = the two-way penetration depth
σ = the extinction coefficient

The coherence scattering model is based on obtaining penetration depth information from the volumetric decorrelation contained in the total coherence (γ_{tot}). The total coherence of TanDEM-X data can be composed of the following components(Krieger et al. 2007):

$$\gamma_{tot} = \gamma_{SNR}\gamma_{Quant}\gamma_{Azimuth}\gamma_{Range}\gamma_{Geo}\gamma_{Temp}\gamma_{Vol} \quad (2)$$

Where γ_{SNR} = noise decorrelation
γ_{Quant} = quantization errors decorrelation
$\gamma_{Azimuth}$ = azimuth/range ambiguities decorrelation
γ_{Range} = baseline decorrelation
γ_{Geo} = ambiguities decorrelation
γ_{Temp} = temporal decorrelation
γ_{Vol} = volumetric decorrelation

γ_{Vol} is the coherence loss caused by volume scattering within the scatterer, which includes penetration depth information. During data processing, correct processing steps such as alignment, filtering, etc. can well compensate the γ_{Quant}, $\gamma_{Azimuth}$, γ_{Range}, γ_{Geo}, and in the standard mode of the TanDEM-X system, $\gamma_{Temp} = 1$ (Krieger et al. 2007). The signal-to-noise ratio decoherence is caused by various noises in

the SAR system and can be compensated for by the following equation:

$$\gamma_{SNR} = \frac{1}{\sqrt{\left(1+\frac{1}{SNR_{TDX}}\right)\left(1+\frac{1}{SNR_{TSX}}\right)}} \quad (3)$$

$$\mathrm{SNR} = \frac{\sigma_0 - \mathrm{NESZ}}{\mathrm{NESZ}} \quad (4)$$

Where SNR = signal-to-noise ratio
NESZ = equivalent zero signal-to-noise ratio

Therefore, the final the volumetric decorrelation can be expressed by the total coherence and temporal decorrelation:

$$\gamma_{\mathrm{vol}} = \frac{\gamma_{\mathrm{tot}}}{\gamma_{\mathrm{SNR}}} \quad (5)$$

Dall (Dall 2007) investigated the relationship between coherence and penetration depth and elevation bias in the literature. It is proposed that when the penetration depth is much smaller than the ambiguity height, the values of penetration depth and elevation bias are approximately equal. Through error analysis, it is suggested that elevation bias is more robust compared to penetration depth. The paper provides a function for penetration depth (elevation bias) with the phase normalized interferometric coherence:

$$\mathrm{d_p} = \angle\gamma / \mathrm{k_{zVol}} \quad (6)$$

Where $\mathrm{k_{zVol}}$ = the vertical wavenumber in the volume

The vertical wavenumber and ambiguity height can be converted into each other. The ambiguity height refers to the height that produces a phase difference of 2π, and its expression is as follows(Rizzoli et al. 2017a):

$$\mathrm{H_a} = \frac{\lambda \mathrm{R} \sin\theta}{\mathrm{B_\perp}} \quad (7)$$

$$\mathrm{H_{aVol}} = \mathrm{H_a}\frac{\cos\theta_\mathrm{r}}{\cos\theta\sqrt{\varepsilon}} = \frac{2\pi}{\mathrm{k_{zVol}}} \quad (8)$$

Where $\mathrm{H_a}$ = the ambiguity height
λ = wavelength
R = the slant range distance
θ = the angle of incidence
θ_r = the angle of refraction
$\mathrm{B_\perp}$ = the vertical baseline
$\mathrm{H_{aVol}}$ = the ambiguity height in the volume
ε = permittivity

The premise for constructing the coherence scattering model is to build a model describing the complex internal structure of snow. Fischer developed models to simulate the penetration depth of InSAR signals at different frequencies, using the UV model and Weibull model to simulate the vertical backscattering profile of snow(Fischer et al. 2020). In this paper, to simplify the model, the snow layer is regarded as a medium with uniform scattering properties, and the UV model is adopted as the vertical distribution of backscattering function. The coherence of a uniform scatterer is known to be:

$$\gamma = \frac{1}{2} + \frac{1}{2}\frac{1-\mathrm{j}2\pi\mathrm{d_p}/\mathrm{H_{aVol}}}{1+\mathrm{j}2\pi\mathrm{d_p}/\mathrm{H_{aVol}}} \quad (9)$$

The correspondence between coherence magnitude and coherence phase can be obtained from the geometrical conditions of the above equation:

$$\angle\gamma = -\mathrm{sgn}(\mathrm{H_{aVol}})\arctan\left(\sqrt{|\gamma|^{-2}-1}\right) \quad (10)$$

In general, the penetration depth information can be obtained from coherence magnitude and coherence phase respectively. However, because of the high sensitivity of InSAR phase information to objects’ height, even a tiny phase error will have a large deviation, so only using phase to estimate the penetration depth is not reliable enough (Liu et al. 2021). The final expression for the penetration depth is Eq 11:

$$\mathrm{d_p} = -\frac{|\mathrm{H_{aVol}}|}{2\pi}\arctan\left(\sqrt{|\gamma_{\mathrm{Vol}}|^{-2}-1}\right) \quad (11)$$

3 Results and Discussion

In this paper, the original TDX/TSX SAR images are subjected to data preprocessing, which includes image registration and generation of intensity maps, etc., and the SAR intensity image after geocoding are shown in Figure 4. The value of backward scattering of snow is related to the particle size of snow, snow thickness and humidity. Because the top layer of this region is covered with thicker and finer-grained snow, and the unique local climate of the plateau glaciers results in slightly lower snow humidity in this area, ultimately leading to a slightly lower backscatter coefficient in the study area compared to surrounding low-altitude areas，as shown in figure 4.(Awasthi et al. 2022).

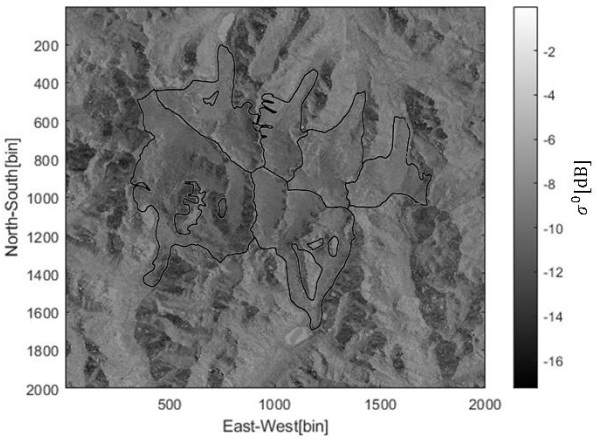

Figure 4. The SAR intensity image

To obtain the volumetric decoherence containing penetration information, coherence of the image needs to be calculated. Following the calculation method of Eq 5 mentioned in the previous chapter, the coherence results can be computed as shown in Figure 5. As illustrated in Figure 5, in the study area, the coherence in high altitude regions is generally higher. The coherence in the region with elevations between 5800-6000m is concentrated above 0.8, while in regions below 5600m elevation, and even lower elevations, the coherence is generally between 0.5-0.7. High coherence indicates that there were no significant changes in the area during the data acquisition period. The higher altitudes typically have lower temperatures, which are more favorable for the persistence of snow. Therefore, in regions with higher altitudes, the coherence is greater. Moreover, the coherence of the windward and leeward slopes is also different. In this research area, the wind is mainly from the southeast in winter(Chu et al. 2023). Therefore, the coherence on the windward slopes to the east will be lower than on the leeward slopes. Moreover, influenced by altitude factors, there will be a

boundary line of high and low coherence at the junction of windward and leeward slopes.

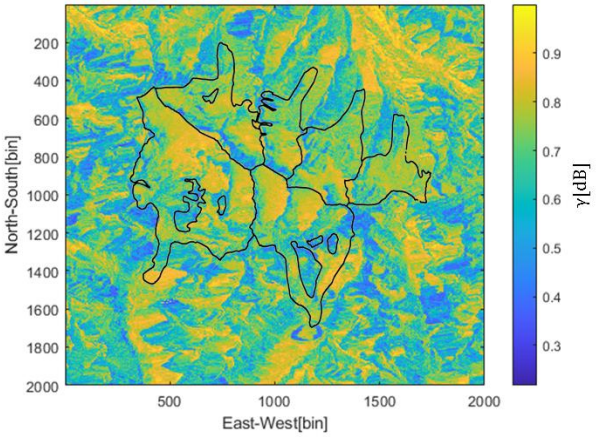

Figure 5. The coherence map

To acquire penetration depth results, besides obtaining the coherence, it is also necessary to acquire the ambiguity height in the volume (H_{aVol}). By calculating H_{aVol} using Eq 8, the acquisition of the dielectric constant is also a difficult task, provided that the basic parameters of the satellite (e.g., wavelength, vertical baseline, angle of incidence, etc.) are known. The effect of the dielectric constant on the penetration depth can be compensated by the change in the incidence angle, so the effect of the change in the dielectric constant of snow on the penetration depth is negligible (Huang et al. 2021), so $\varepsilon = 1.763$ is taken(Matzler 1996). The final H_{aVol} calculations are shown in Figure 7. Figure 6 shows the ambiguity height in the air, which is primarily distributed around -47.5 to -43.5 meters due to the influence of the incidence angle and vertical baseline. Figure 7 illustrates the ambiguity height in the volume that include this portion of scattering and refraction. The ambiguity height value determines the vertical resolution, with a smaller absolute value of the ambiguity height leading to lower vertical resolution. From Figure 7, it can be observed that the H_{aVol} in the study area mainly ranges from -40 to -20 meters, in which the H_{aVol} is overestimated in the area with large elevation changes. Furthermore, comparing the coherence with the ambiguity height in the volume map reveals that the areas where coherence is less than 0.35 coincide with regions where H_{aVol} exceeds -10 meters. These overlapping regions correspond to the boundaries between glaciers. This is because the edge of the glacier is the most dynamic areas, prone to glacier melting at low altitudes and undergoing movements like compression and collision between glaciers. The instability of the glacier induces alterations in the motion of the overlying snow layer, thereby impacting the calculation of penetration depth. For the sake of accuracy in subsequent calculations, the regions where H_{aVol} exceeds -10 meters are being masked.

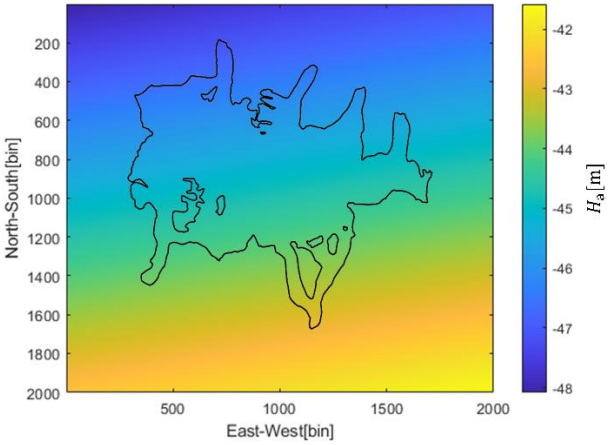

Figure 6. The ambiguity height map

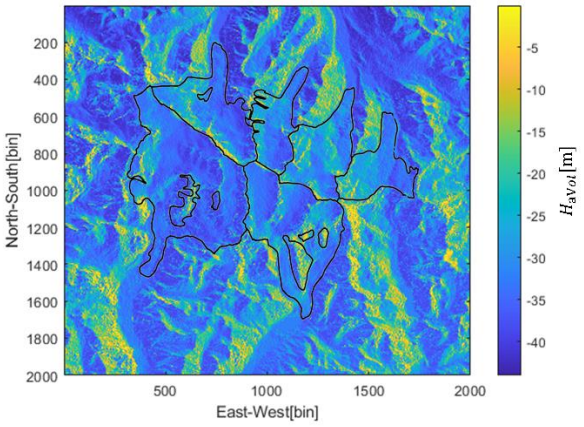

Figure 7. The ambiguity height in the volume map

Based on the aforementioned results, utilizing Eq 11 in combination with coherence and H_{aVol}, the penetration depth in snow can be acquired. The resulting figure is illustrated in Figure 8. According to the statistical graph in Figure 9, it is evident that the average penetration depth in the study area is -3.671 meters, with a standard deviation of 0.918 meters. The penetration depth values in the study area are concentrated between -2.753 meters and -4.589 meters. These calculated results exhibit good consistency with previous studies(Rizzoli et al. 2017b; Rott et al. 2021).

As can be seen in Figure 8, it can be observed that the penetration depth is deeper in areas with low coherence. This is because with greater penetration depth, there is stronger volume scattering, leading to a weakening of the corresponding echo signals, thus resulting in lower coherence. It can be observed that the penetration depth in regions with significant elevation changes (the red boxed part of the figure 8) is deeper compared to areas with relatively flat terrain (the blue boxed part of the figure 8). This is because in areas with steeper slopes, the stability of the snow cover in the upper layers is poorer, leading to slightly lower local coherence. Therefore, in the calculation of the coherence scattering model, the accurate extraction of volumetric decorrelation becomes particularly important. It can be seen from the statistics that the deepest penetration depth value exceeds 7m, while the shallowest place is only 1m. This discrepancy may be attributed to the assumption in this paper that snow is a uniform scattering scatterer. However, in reality, due to various factors such as temperature, humidity,

precipitation and other factors, the internal conditions of snow are complex and variable. This systematic bias in calculating penetration depth is inevitable when considering snow as a homogeneous scattering medium.

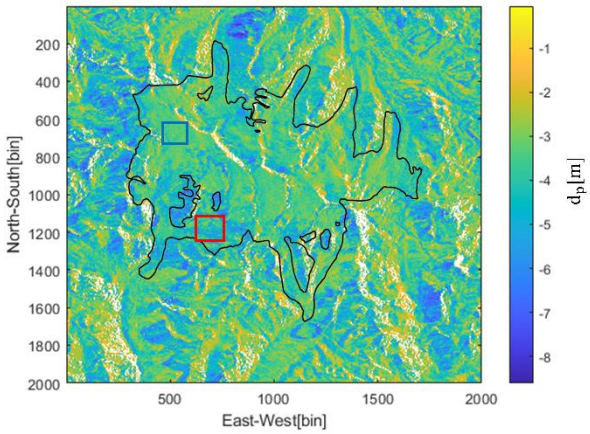

Figure 8. The penetration depth map

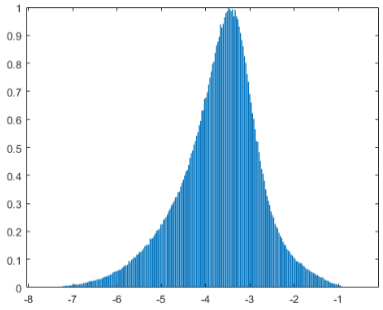

Figure 9. The histogram of the penetration depth

4 Conclusions

In this paper, the coherence scattering model based on magnitude of volumetric decorrelation was constructed to obtain the penetration depth in snow. Additionally, this paper also analyses the link between external factors (e.g. climate, topography, dielectric constant) and interference parameters. And factors affecting the depth of penetration are analyzed. To validate the effectiveness of this model in detecting snow on glaciers in the Tibetan Plateau, the coherence scattering model was applied for the first time to snow in the Tibetan Plateau, utilizing TDX/TSX InSAR data from glacier groups such as the Zuhuixue Glacier in the southeastern part of the plateau. The model computed the volumetric decoherence, which includes refraction and scattering information when microwaves into the scattering body, and described the ambiguity height in the scattering that represents snow properties, thereby further calculating the penetration depth. The final results indicated an average penetration depth of -3.671 meters in the X-band within the snow, showing good consistency with historical research.

In future research, we plan to establish a coherence scattering model based on non-uniform scattering media to calculate the penetration depth of more complex real-life scenarios. Additionally, in order to obtain deeper penetration depth and richer information about the interior of scatterers, the next step involves considering the application of long-wave InSAR in the coherence scattering model.

Acknowledgements

The TDX/TSX data was generously supplied by Professor Yushan Zhou and his team. Other data used in this study were graciously provided free of charge by The National Tibetan Plateau Data Center (TPDC).

References

Awasthi, S., Varade, D., Thakur, P.K., Kumar, A., Singh, H., Jain, K., & Snehmani 2022. Development of a novel approach for snow wetness estimation using hybrid polarimetric RISAT-1 SAR datasets in North-Western Himalayan region. *Journal of Hydrology, 612*, 17

Benedikter, A., Rodriguez-Cassola, M., Betancourt-Payan, F., Krieger, G., & Moreira, A. 2022. Autofocus-Based Estimation of Penetration Depth and Permittivity of Ice Volumes and Snow Using Single SAR Images. *IEEE Transactions on Geoscience and Remote Sensing, 60*, 15

Chu, D., Liu, L.S., & Wang, Z.F. 2023. Spatial Distribution of Snow Cover in Tibet and Topographic Dependence. *Atmosphere, 14*

Dall, J. 2007. InSAR Elevation Bias Caused by Penetration Into Uniform Volumes. *IEEE Transactions on Geoscience and Remote Sensing, 45*, 2319-2324

Eppler, J., & Rabus, B.T. 2022. The Effects of Dry Snow on the SAR Impulse Response and Feasibility for Single Channel Snow Water Equivalent Estimation. *IEEE Transactions on Geoscience and Remote Sensing, 60*, 23

Fischer, G., Papathanassiou, K.P., & Hajnsek, I. 2020. Modeling and Compensation of the Penetration Bias in InSAR DEMs of Ice Sheets at Different Frequencies. *IEEE Journal of Selected Topics in Applied Earth Observations and Remote Sensing, 13*, 2698-2707

Guo, W.Q., Liu, S.Y., Xu, L., Wu, L.Z., Shangguan, D.H., Yao, X.J., Wei, J.F., Bao, W.J., Yu, P.C., Liu, Q., & Jiang, Z.L. 2015. The second Chinese glacier inventory: data, methods and results. *Journal of Glaciology, 61*, 357-372

Huang, L.Q., Fischer, G., & Hajnsek, I. 2021. Antarctic snow-covered sea ice topography derivation from TanDEM-X using polarimetric SAR interferometry. *Cryosphere, 15*, 5323-5344

Krieger, G., Moreira, A., Fiedler, H., Hajnsek, I., Werner, M., Younis, M., & Zink, M. 2007. TanDEM-X: A satellite formation for high-resolution SAR interferometry. *IEEE Transactions on Geoscience and Remote Sensing, 45*, 3317-3341

Li, C., Jiang, L.M., Liu, L., & Wang, H.S. 2021. Regional and Altitude-Dependent Estimate of the SRTM C/X-Band Radar Penetration Difference on High Mountain Asia Glaciers. *IEEE Journal of Selected Topics in Applied Earth Observations and Remote Sensing, 14*, 4244-4253

Mahmoodzada, A.B., Varade, D., & Shimada, S. 2020. Estimation of Snow Depth in the Hindu Kush Himalayas of Afghanistan during Peak Winter and Early Melt Season. *Remote Sensing, 12*

Matzler, C. 1996. Microwave permittivity of dry snow. *IEEE*

Transactions on Geoscience and Remote Sensing, 34, 573-581

Patil, A., Singh, G., & Rüdiger, C. 2020. Retrieval of Snow Depth and Snow Water Equivalent Using Dual Polarization SAR Data. *Remote Sensing, 12*, 11

Rizzoli, P., Martone, M., Gonzalez, C., Wecklich, C., Tridon, D.B., Bräutigam, B., Bachmann, M., Schulze, D., Fritz, T., Huber, M., Wessel, B., Krieger, G., Zink, M., & Moreira, A. 2017a. Generation and performance assessment of the global TanDEM-X digital elevation model. *Isprs Journal of Photogrammetry and Remote Sensing, 132*, 119-139

Rizzoli, P., Martone, M., Rott, H., & Moreira, A. 2017b. Characterization of Snow Facies on the Greenland Ice Sheet Observed by TanDEM-X Interferometric SAR Data. *Remote Sensing, 9*, 24

Rott, H., Scheiblauer, S., Wuite, J., Krieger, L., Floricioiu, D., Rizzoli, P., Libert, L., & Nagler, T. 2021. Penetration of interferometric radar signals in Antarctic snow. *The Cryosphere, 15*, 4399-4419

Xu, Y., Lu, Z., Bürgmann, R., Hensley, S., Fielding, E., & Kim, J. 2023. P-band SAR for ground deformation surveying: Advantages and challenges. *Remote Sensing of Environment, 287*

Zhang, Y.H., Peng, X., Xie, Q.H., Du, Y.N., Zhang, B., Luo, X.M., Zhao, S.B., Hu, Z.T., & Li, X.W. 2023. Forest height estimation combining single-polarization tomographic and PolSAR data. *International Journal of Applied Earth Observation and Geoinformation, 124*

Zhao, Q., Xie, Q., Peng, X., Lai, K., Wang, J., Fu, H., Zhu, J., & Song, Y. 2024. Understanding the Temporal Dynamics of Coherence and Backscattering Using Sentinel-1 Imagery for Crop-Type Mapping. *IEEE Journal of Selected Topics in Applied Earth Observations and Remote Sensing, 17*, 6875-6893

Zhou, Y., Li, X., Zheng, D., & Li, Z. 2022. Evolution of geodetic mass balance over the largest lake-terminating glacier in the Tibetan Plateau with a revised radar penetration depth based on multi-source high-resolution satellite data. *Remote Sensing of Environment, 275*